교육학석사 학위논문

The study on the oxidation of DNA-Silver nanodots and its application

DNA에 둘러싸인 은 나노닷의 산화 특성에 대한 연구 및 적용

2014 년 6 월

서울대학교 대학원

과학교육과 화학전공

박 순 영

The study on the oxidation of DNA-Silver nanodots and its application

지도교수 Yu, Junhua

이 논문을 교육학석사 학위논문으로 제출함

2014 년 6 월

서울대학교 대학원

과학교육과 화학전공

박 순 영

박순영의 교육학석사 학위논문을 인준함

2014 년 6 월

위 원 장 _____ (인)

부위원장 _____ (인)

위 원 _____ (인)

Abstract

The study on the oxidation of DNA-Silver nanodots and its application

Soonyoung Park

Department of Science Education

(Major in Chemistry)

The Graduate School

Seoul National University

Fluorescence has been progressively adapted toward *in vivo* molecular imaging recently because of their high sensitivity and selectivity, which make it possible to detect target at single molecule level with a high temporal resolution, in optimized system. To achieve efficacy of fluorescence imaging, a proper fluorescence probe is essential. ssDNA encapsulated Ag NDs are most attractive emerging fluorophores, because of their excellent photophysical properties and reasonable biocompatibility. However accurate structures and synthetic mechanisms of DNA-Ag NDs are still not clear. Therefore analyzing the

response of DNA-Ag NDs in the process of oxidation gives us better understanding of DNA-Ag NDs. We examined the oxidation process of NDs by using red emissive DNA-Ag ND molecules in the presence of various reactive oxygen species. In addition, with discovered oxidative properties, we have developed ratiometric luminescence probes and new form of imaging process.

Key words: DNA, Ag NDs, Ratiometric, Hydrogen peroxide, Hypochlorite, Glucose oxidase

Student number: 2011-21578

Contents

List of Figures

List of tables

I. Introduction

1.1. Molecular imaging

1.1.1. What is the molecular imaging?

Molecular imaging is defined as "the *in vivo* characterization and measurement of biological process at the cellular and molecular level."[1] Whereas conventional bio imaging modalities have been focusing on getting anatomic structure or diagnostic information,[2] molecular imaging is considered as noninvasive, quantitative, and repetitive imaging of targeted macromolecules and biological processes in living organisms.[3]

Since the use of energy transmitted through the living organism, X-ray and CT (Computed Tomography) are referred to as transmitted imaging technique. For receiving reflected high frequency sound pulses, US (Ultrasonography) is regarded as a reflection imaging technique.[4] The images of those two categories mainly portray anatomic features,[2] and are applied for the observation of the altered anatomy.[5, 6] Unlike the previous modalities, MRI (Magnetic Resonance Imaging) focused on to explore the physiological changes. But it is also largely related to assess disease diagnosis, surgical approach, and therapeutic response.[7]

Those current biomedical modalities are based on anatomic changes or physiologic changes that are a resulted symptom from the molecular changes that truly underlie disease.[8]

Therefore the true meaning of molecular imaging emphasized here is method to image specific molecular pathways *in vivo* at the molecular or cellular level, particularly those that are key targets in disease process.[9] Direct imaging of these molecular changes will allow much earlier detection and 'real time' monitoring of disease as well as investigating the efficacy of drugs.[8, 10]

Usually even the normal CT, US, and MRI are also considered as modalities of molecular imaging, but when we focus on the causes and prevention discovery of the occurrence of the disease, PET and Optical imaging are possible to be included under molecular imaging in the true sense of the term.[11]

1.1.2. PET (Positron Emission Tomography)

PET (Positron Emission Tomography) is a major part of the nuclear medicine, functional imaging technique. In nuclear medicine image, radioactive component is injected into the human body by intravenous injection, inhalation or ingestion.[12] This radiotracer selectively moves into organ or other areas of the human body and then each molecule of a substance labeled with a radioactive

element emits gamma (γ) rays in accordance with the density of the compound.[13]

PET records high-energy γ-rays emitted from the subject that labeled with positron-emitting isotope which is capable of producing two γ-rays through emission of a positron from its nucleus.[10] PET can perform functional imaging of physiological processes with exquisite specificity if an appropriate radiolabeled tracer analogue exists.[14] Frequently used positron-emitting isotopes are produced in a cyclotron, and most of them have relatively short half-lives.[15] High cost from the frequent using of an expensive cyclotron is one of the critical limitation of PET modality.[14] In addition, while the sensitivity of PET is relatively high, it has a low spatial resolution.[16]

1.1.3. Optical imaging

Optical imaging techniques have already been used widely for *in vitro* applications in molecular and cellular biology. The essential issue for an extension of traditional method toward noninvasive *in vivo* imaging has been defined as how to well detect light photons emitted from the body of living organism.[15] It is widely appreciated that optical imaging can't defeat in terms of spatial resolution with anatomical imaging technique (x-radiography, US and MRI),[17] nonetheless, optical imaging also offers relatively high spatial resolution

that is greater than limit of light diffraction.[1, 17] Moreover, optical imaging offers several distinct advantages.[18] Such as a sensitivity to functional changes which makes possible real-time functional readouts in animal models,[19] the fact that optical imaging does not have strong safety concerns unlike the other medical imaging modalities do,[20] a considerably low cost and being easy to operate equipment.[21]

1.1.3.1. Strategies of optical imaging

Even though Optical imaging can be widely classified into two categories, fluorescence- and non-fluorescence-one, [21-24] what we are more interested in here is fluorescence based imaging techniques. Fluorescence has been progressively adapted toward *in vivo* molecular imaging recently[25] because of their high sensitivity and selectivity.[26] With optimized system, the fluorescence spectroscopy can detect single molecules longitudinally.[27]

Typical limitation of fluorescence optical imaging was tissue penetration and light absorption.[1, 28, 29] Excitation in the UV region can cause tissue damages, whereas over 900nm wavelength where water in the body of living organism mainly absorbs light, it can cause strong background noise. Besides, in the visible region, blue and green excitation lights make a large scattering,[30] and

consequentially have poor tissue penetration which enables superficial analysis only. [11]

To overcome these shortcomings, firstly NIR fluorescence imaging was adopted.[31] The confocal microscopes have advantages in terms of their increased axial resolution which allows light to travel into deeper tissues by using a spatial pinhole to eliminate out-of-focus light.[32] Moreover they can make three dimensional reconstruction from the obtained images.[33, 34]

Two-photon microscopy imaging which is developed from the quantum entanglement[35] achieved the tissue penetration depth up to one-milimeter,[36] producing three dimensional information. At the same time it is not hazardous because the NIR (near-infrared) light used in excitation does not have strong energy as ultraviolet.[37] Additionally, various attempts to combine several technologies, such as fluorescence mediated tomography (FMT), FMT-CT, FMT-MRI, fluorescence PET,[38] etc., have been progressing in order to make use of complementary advantages of them. [21] .

In another perspective, the attractive progress in instrumentation and methodology of fluorescence optical imaging are made by designing better imaging probes.[3, 39]

1.2. Fluorophores

Here, I firstly want to introduce the basic principles of fluorescence, before examine probes in detail for better understanding. I will previously leave it clear that the following descriptions in this chapter are constituted with reference to "Fluorescence applications in biotechnology and the life sciences" by Ewa M. Goldys[25] and "Physical chemistry" by PW. Atkins.[40]

1.2.1. Photoluminescence

The definition of luminescence is "a spontaneous emission of radiation from an electronically excited species (or from a vibrationally excited species) not in thermal equilibrium with its environment".[41] In particular, photoluminescence is the emission of light induced "from direct photoexcitation of the emitting species".[41] Fluorescence and phosphorescence are well-known forms of photoluminescence.[42]

1.2.1.1. Basic principles of photoluminescence

Light is a form of electromagnetic radiation that behave like waves travelling at the speed of light ($c=3.0\times10^{8}$ m/s). The wavelength (λ), frequency (ν), and

speed (c) of light have mathematical relationship defined as below.

$$\nu = \frac{c}{\lambda}$$

Early 20th century, Planck supposed that the energy of an electromagnetic wave could not have any value but was quantized with a standard unit of light which is called a photon as demonstrated following equation.

$$E = h\nu$$

Where E means the energy of light, h is called the planck constant (h= 6.626×10^{-34} J·s).

When a molecule is placed in an electric field, by theory of 'Wave-particle duality',[43] molecule also has specific resonant frequencies at which an associated energy level. *Vibrational states* represent to particular resonant frequencies of the atoms in a molecule vibrating together. In *Electronic states*, electrons make transitions back and forth in a molecule between resonant frequencies that correspond to distinct orbitals. What needed to be considered in optical spectroscopy are electronic states of valence electrons.

When molecules in their 'ground state' absorb photons, alterations in the electronic and vibrational states can occur.[44] The absorbed energy moves an electron into an 'excited state' where releases its energy soon because it is unstable. The emitted light (photon) from excited state back to ground state is known as '*fluorescence*' or '*phosphorescence*'.

Usually molecules absorb or emit one photon at a time, but under conditions of very intense radiation, two or more photons can be absorbed simultaneously only with the half of the frequency.[26]

1.2.1.2. Fluorescence and phosphorescence

The spin of electrons is associated with specific energetic states. According to '*the Pauli principle'*, all energy levels (orbitals) only can accommodate two electrons with opposite spin direction. Therefore the most stable molecular states have zero total electrons spin quantum numbers. Although an electron has been excited, because its spin direction could not be flipped during short excitation interval (*Wigner rule*),[45] still total spins are zero. This is called as 'singliet state'.

On the other hand, if the direction of excited electron's spin is changed, so that the total spin quantum numbers became '1', the magnetic energy levels of that molecule are separated into three sublevels, likewise when total angular momentum quantum number becomes 1, we can get three *p* orbitals. Therefore it is called as 'triplet state'. Note that, triplet excitation states are more stable than singlet in energy, because three adjacent orbitals are preferred as they can reduce electron repulsion.[46] Therefore electrons at which triplet excitation state can stay much longer than singlet excitation state before turning back to their ground state.

We call the former that emissive light from singlet excited state as '*Fluorescence*', and the latter that from triplet state as '*Phosphorescence*'.

A '*Jablonski diagram*' is a useful depiction of the details of the excitation and emission process.[44] As shown below, Once electrons excited from their ground state, they can choose not only radiative ways but also non-radiative paths for losing their unstable high energy. Through *VR* (Vibrational Relaxation), excited molecules emit their energy by heat until they left in the lowest vibrational state of S_1. Whereas in *IC* (Internal Conversion), excited state converted to a high vibrational state of S_0.

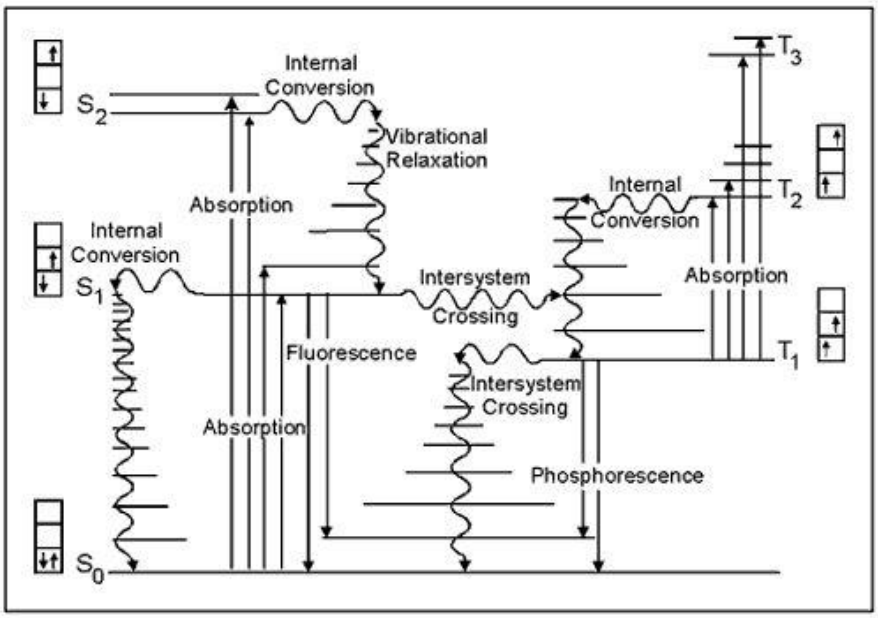

Figure 1. Jablonski diagram demonstrate the electronic states of molecules and transitions between them.

Lastly *ISC* (Intersystem Crossing) is non-radiative transfer between singlet and triplet states not by absorption or emission of light, but by collisions with surrounding molecules.

As described above, when electrons have been excited by light absorption, it can occur diverse processes. The *quantum yield* $\emptyset_i$ for process *i* mean the rate of process *i* (k_i) divided by the sum of all rates. In brief, it is the fraction of certain process among all process.

$$\emptyset_i = \frac{k_i}{\Sigma k}$$

And the average time that valence electron of molecule stays in its excited state before re-emitting is called the *lifetime* and denoted by tau (τ).

1.2.2. What is good fluorophore?

At ultralow pressure, the gas phase single molecule experiments have been done commonly. But in the condensed phase, it has been started only since late 1980's.[47, 48] Fluorescence is a convenient method of detecting single molecule in the condensed phase mainly due to their high sensitivity. However in the life organism, it is not straightforward issue, since there already have been a lot of fluorescent molecules called autofluorescence.[49-51] In order to observe necessary single molecule efficiently, signal distinguishable from the background is

necessary. Adding signals that make easy to detect target single molecule is labelling and added signal is called probe.[52] Here, the molecules that are used as probe by their fluorescence properties are fluorophore.[44] In this section, I want to discuss about what conditions are required to good fluorophore and which fluorophores have been widely used.

1.2.2.1. Required photo physical properties of good fluorophore

There are several characteristics of successful fluorophore for molecular imaging including proper wavelength, brightness, photostability, and biocompatibility.[11]

The optimal excitation wavelength of a fluorophore is in the deep red or near-infrared range in order to fulfill both good tissue penetration depth and low background noise.[53] As I mentioned above, it is very important to choose proper wavelength that minimize background noise and harmness from light irradiation.

The ability to emit light in a particular environment is referred as brightness (B_e) which is described by the equation below.

$$B_e = \emptyset_f \cdot \varepsilon$$

Where $\emptyset_f$ stands for quantum yield of fluorescence process at certain excitation/emission wavelength, and ε imply molar extinction coefficient (or

molar absorption coefficient) ($M^{-1} \cdot cm^{-1}$) which determine the ability of absorption light.

Then, the photostability is associated with quenching of fluorescence and photobleaching. Quenching is the other non-radiative process of losing excited energy. So called quencher can overlap their aromatic ring structures with original fluorophore. In this process concerned fluorophores are deactivated by donating electrons to quencher. Virtue of this property can be applied to FRET (fluorescence resonance energy transfer).[54] However when it is not properly utilized, just become a main factor of lowering photophysical stability. The other part known as photobleaching is related to intersystem crossing. In their triplet states, molecules may react with other molecules leading to formation of stable complexes that lead to deactivation of excited state without the emission of light.[55]

Lastly with regard to biocompatibility, to be applied to bioimaging, fluorophores should be soluble in relevant buffers, for example cell culture media or body fluids, fundamentally.[56] It is also needed to have proper functional groups for conjugation with specific tissues. Especially in order to reach to target tissues safely overcoming the resistance circulation system, digestive organs, and immune systems, we should consider a lot of things, such as probe's size, toxicity, surface properties (charge, hydrophilicity, coating characteristic, etc.), density,

pH, etc..[57-59]

Developing bright fluorescent probes is main target for achieving better optical imaging quality.[60, 61] At the same time, in terms of cellular imaging, the conjugation of a specific targeting group and the selective response to an analyte is also the key to an effective probe design.[39, 62] To conclude, for being a good fluorophore, they should satisfy all of these criteria largely devided into photophysical property and biocompatibility.

1.2.3. Widely used fluorophores

1.2.3.1. Organic fluorophores

In fluorescence microscopy, the kind of the most widely used probe is organic fluorophore. Fluorescence emission occurs from organic molecules with conjugated double-bond system.[25, 52] In the beginning of medical application of fluorescence probe, scientists used naturally occurring fluorescence molecules. But later scientist developed lots of synthetic chemical fluorophores or genetically encoded protein fluorophores. For there is a lot of commercially used organic fluorophores, we should carefully select what is the suitable wavelength, proper surface properties fitted target tissues.[49] The most powerful benefit of

organic fluorephores is the biocompatibility.

Even though numerous bio imaging probes have been developed in the past few decades,[63] the organic fluorophores used for signaling still suffer from low probe brightness, poor photostability, and oxygen bleaching.[64] Consequently, the creation of fluorophores with improved photophysical properties is still in high demand.[60, 61]

1.2.3.2. Quantum dots

Semiconductor quantum dots (QDs) are inorganic nanocrystals made from II/VI, III/V and Ⅳ/Ⅳ atoms of periodic table, such as CdSe, CdTe, InP and InAs.[22, 61] With decrease of bulk metals' size into nanometer scale, discrete energy levels are appeared. QDs make use of fluorescence from transitions of electrons between HOMO (the highest occupied molecular orbital) and LUMO (the lowest unoccupied molecular orbital).[40]

QDs appeared excellent photophysical properties that overcome the drawbacks of organic fluorophores.[61, 65] Even though QDs fluorescence quantum yield is similar to organic fluorophores, but for excellent molar extinction coefficient, QDs brightness is brighter than organic fluorophores over one order magnitude. Then QDs markedly reduced photobleaching rate.[66] Consequently, QDs have

advantageous photophysical properties, such as high brightness, large absorption cross-sections, and outstanding photophysical stability.

However QDs are not sufficiently biocompatible due to their large size, intermittent photon emission, tendency to aggregate, and intrinsic toxicity of heavy metals. [67]

1.3. DNA encapsulated silver nanodots

Ag NDs (Ag nanodots) are small, few-atom clusters that exhibit discrete electronic transitions and strong photoluminescence.[68, 69] After the report of the first stable silver nanodots in aqueous solution in 2002,[70] Initially, Ag clusters were prepared in noble gas matrices due to their vulnerability to oxidation.[71] However, the vulnerable property of unprotected noble metal clusters to oxidative damage requires more intensive protections.[71] Later, many scaffolds have been developed. As a specific example, poly(acrylic acid),[72] short peptides,[73] single-stranded DNA (ssDNA), and thiolated small molecules are applied widely as protection groups.[69] Applying various protection groups has markedly improved their stability in aqueous solution, leading to the synthesis of a series of spectrally-pure AgNDs with emission wavelengths ranging from the blue to the near-IR.[70, 74]

1.3.1. Advantages of DNA-Ag NDs

Among those scaffolds, ssDNA stabilization has induced the best photophysical characteristics of Ag NDs. For DNA-Ag NDs show not only high one- and two- photon molar extinction coefficients, but also high emission (fluorescence) quantum yields, subsequently have high brightness. Especially its superior two-photon absorption coefficients are great advantage, for as mentioned above, two-photon fluorescence spectroscopy is one of the most powerful modalities in fluorescence molecular imaging. Moreover DNA-Ag NDs have outstanding photostability which means that they not only don't show blinking, but also have reasonably good fluorescence lifetime. DNA-Ag NDs have small overall size about 5nm or below, water soluble, nontoxic with noble metal silver that is commonly used in human life.[64, 73, 75-78].

Consequently, we can consider DNA-Ag NDs as fluorescence probe which has excellent photophysical properties comparable to semiconductor QDs and much closer biocompatibility to Organic fluorophore. For these reasons, DNA-encapsulated AgNDs have been attracting huge attention in fluorescence molecular imaging.[68, 77, 79-81]

1.3.2. Undisclosed DNA-Ag NDs emission mechanism

The exact structures and the transitions between various DNA-AgNDs are still under debate.[82, 83] If the process is composed by effective control over the whole interactions between the ingredients and entropic effect, then the resulting structure will be ordered. But in terms of DNA-Ag NDs, it remains challenging for they use self-assembly as synthetic systems.[84]

Even in this case, if we could get crystral structure of DNA-Ag NDs, it can be identified via x-ray diffraction.[85] Unfortunately, the fluorescent silver nanodots crystal is still not reported. Besides, purification of DNA-Ag NDs becomes more difficult due to the low DNA-Ag NDs synthetic yield and numerous possible complexes between silver and protection groups. As a result, although it is not directly interpreted to silver nanodots structure, deciphering of DNA-Ag NDs structure is mostly based on photospectroscopy information.[68]

1.4. What happens in oxidation of DNA-Ag NDs

As mentioned above, there is a limitation to determine the structure of DNA-silver NDs just through their photophysical spectroscopy information. However, under this circumstance, analyzing the response of DNA-Ag NDs appearing in

the process of oxidizing using various oxidizing agent is meaningful. From this observation, it is possible to infer the DNA-Ag NDs' structures and reaction mechanisms *via* acquired clue in oxidation of DNA-Ag NDs. At the same time we can make use of the characteristics of the oxidative DNA-Ag NDs to develop specific probe for certain oxidant.

1.4.1. Oxidation of DNA-Ag NDs

The DNA encapsulated silver NDs' red emitters were considered to be fully-reduced species. Ripening from red emitters results in typically the blue,[86] the green,[74] or the yellow AgNDs.[74, 79] Oxygen was believed to play a role in such processes and especially the blue emitter was proposed to be a species oxidized directly from the red emitters.[86]

However, it was ignored that the creation of such derived emitters was due to the rearrangement of red emitters, not just the simple decrease in nanodot size. Herein we examined the reactions of various DNA-Ag NDs in strong oxidizing environments induced by diverse ROS (reactive oxygen species) to trace the link between the red and its derivatives, and found that such processes could be selectively tuned by different ROS.

1.4.2. Applications of oxidative DNA-Ag NDs for specific probe

Hypochlorite (OCl^-) is a major ROS species. Especially in immunological cells, cellular OCl^- is synthesized by myeloperoxidase (MPO)-catalyzed oxidation of chloride ion with hydrogen peroxide (H_2O_2)[87, 88] The regulated generation of OCl^- plays a predominant role during the microbicidal process in the immune system. However, uncontrolled overproduction of OCl^- in phagocytes is regarded as a provoking cause of diseases.[89-94]. Even though it is very important and urgent to explain the pathways of OCl^- generation and its systemic impact, progress is still slow since it is hard to detect transient ROS refluxes.[91]

Sodium hypochlorite is also one of the major active ingredients used as a disinfectant and bleach in some cleaners, together with surfactants, builders, solvents, etc.[95] Even though widely used, excessive hypochlorite may induce neurodegeneration, endothelial apoptosis, ocular irritation, and other tissue damage.[87, 96-99] Chemosensors are indispensable to allow us to obtain the exact concentration of OCl^- with high spatiotemporal resolution. We were tried to develop a different class of OCl^- probe using oxidative DNA-Ag NDs. Prior to evaluating the bio-suitability of our probe, investigated the parameters for accurate detection of hypochlorite and evaluated the derived ratiometric imaging

method by monitoring the concentration of OCl^- in commercially available cleaners.

Meanwhile, we explored the capability of oxidative DNA-Ag NDs as imaging agents in presence of hydrogen peroxide (H_2O_2) with glucose oxidase. As a new strategy, by coupling analyte to glucose oxidase (GOx) we can theoretically detect any analyte with excellent selectivity and greatly improved detection limit *in-vivo*.

The glucose oxidase is an enzyme that catalyzes glucose into hydrogen peroxide and D-glucono-δ-lactone. Looking more closely, GOx needs a cofactor for working as catalyst, flavin adenine dinucleotide (FAD). In the GOx-catalyzed redox reaction, FAD initially accepts electron and is reduced to $FADH_2$. Then $FADH_2$ is oxidized by oxygen (O_2), and then O_2 is reduced to hydrogen peroxide (H_2O_2).[100]

Just as hypochlorite, hydrogen peroxide (H_2O_2) are also involved in a wide range of physiological and pathological processes. Although H_2O_2 produced in normal cellular environments are essential for life, they are harmful when overproduced by exogenous stimulation.[101-104] To stably regulate the amount of H_2O_2 *in-vivo*, it is necessary for *micro*- or *nano*- molar detection capability at least.[105] To meet these needs we designed novel imaging strategy using GOx and oxidative DNA-Ag NDs.

II. Experimental section

2.1. Chemicals

Chemicals. Silver nitrate (99.9999%), sodium hypochlorite, hydrogen peroxide, potassium dichromate, potassium dioxide, Hoechst 33258, harmaline, sodium sulfate, glucose oxidase, biotin 3-sulfo-n-hydroxysuccinimide ester, iron perchlorate, tert-butyl hydroperoxide, tris(2-carboxyethyl)phosphine hydrochloride, sodium borohydride and polyvinyl alcohol were purchased from Sigma-Aldrich and used as received. DNA was purchased from IDT DNA. Avidin modified magnetic nanoparticles were purchased from Fisher Scientific. Hydroxyl radical and alkylperoxy radicals were generated from corresponding amount of hydrogen peroxide or tert-butyl hydroperoxide in the presence of 1 mM iron perchlorate respectively.

2.2. Preparation and measurement of samples

Preparation of silver nanodots. Different silver nanodots emitters were prepared according to published data.[74, 79, 86] Briefly, ssDNA and silver ions were

mixed at a DNA base/Ag+ ratio of 2:1. For chemical reducing, 2~3 hr later NaBH4 was added into the mixture. At that time, the amount of borohydride was optimized to produce maximum blue emitters with a Ag+/NaBH4 ratio of 6/5, slightly lower than the regular NaBH4 dose. Silver nanodots were used as probe a day after chemical reduction of the mixture.

Comparison of photostability. The above mixtures were dropped onto quarts cuvettes for measuring absorbance. Absorption spectra were recorded on a SCINCO S-4100 Scan UV–visible spectrophotometer (Seoul, Korea) at room temperature. Sample was filled onto the glass vial when it was measured on a PTI QuantaMaster™ 30 Plus Phosphorescence/Fluorescence Spectrofluorometer.

Dyes and the blue silver nanodots were mixed with 1% PVA in the presence or absence of 5mM of hydrogen peroxide. The above mixtures were dropped onto a glass coverslip and dried under vacuum for 15 min. The resulting films were imaged under continuous UV excitation on an Olympus IX81 inverted microscope equipped with 60× 1.35 NA objective and Andor Luca CCD camera. The excitation filter was 360-370 band pass and the emission filter BP 460-495.

HRTEM and HPLC-MS spectrometry. HRTEM images were obtained on JEM 3010 high resolution transmission electron microscope at voltage of 300kV. The sample for TEM characterization was prepared by placing a drop of colloidal solution on a carbon-coated copper grid which was dried at room

temperature.

Specific samples were analyzed with HPLC-MS system (acetonitrile/water, ESI-MS system (LCQ)).

III. Results and discussion

3.1. Oxidation properties of DNA-Ag NDs

From the same red peaks of polycytosine protected AgNDs (C24-Ag NDs, λ_{em}=625nm), different kinds of peak shift are generated selectively by ROS oxidation as shown in (Figure 2). As mentioned in introduction part (**1.3.1.**), the reason of this phenomenon has widely believed that it is because of their size decrease, caused by oxidation from the oxygen in the air.[86] However, results shown in Figure 2 bring some conflict from old belief.

Both hydrogen peroxide (H_2O_2) and sodium hypochlorite (NaOCl) quenched the red, meanwhile, a blue emitter (λ_{em}=485nm) was generated with an excitation maximum at 340nm (Figure 2a and d). Under a hydrogen peroxide, the red C24-Ag NDs decreased faster than the generation of the blue emitter (Figure 2b). Higher hydrogen peroxide concentration did not quench the red emission faster, but accelerated the generation of the blue significantly.

Intriguingly, with the sodium hypochlorite, oxidation of the red C24-Ag NDs induced blue emission much faster than the bleaching of the red (Figure 2e), indicating that the blue emitter had been formed before the decay of the red.

If these peak shifts were simply because of reduced size owing to oxidation, their kinetic behavior should have been same in various ROS. But the kinetic data suggested that the blue emitter had been formed before the decay of the red emitter. A simple decrease of the cluster size could not account for the transition from the red to the blue. Therefore we assumed that there are some intermediate states are related.

Besides, another oxidizing agent potassium dioxide (KO_2) which induce superoxide radical can give yellow emission from the same C24-Ag DNs (Figure 2g). Note that, following the addition of potassium dioxide, the red emission intensity increased at the first and then about 1hr later started to decrease continuously (Figure 2h). Such a phenomenon was likely due to the generation of hydrogen from hydroperoxy radicals, which initially reduces precursors of the red emitter. Being strong oxidizing agents,[106, 107] hydroxyl radical and alkylperoxy radicals quenched most of the emissions (Figure 2j and k), but interestingly, the green lasted longer and the emission intensity ratio (I525/I625) correlated the concentration of hydroxyl radical (Figure 2l).

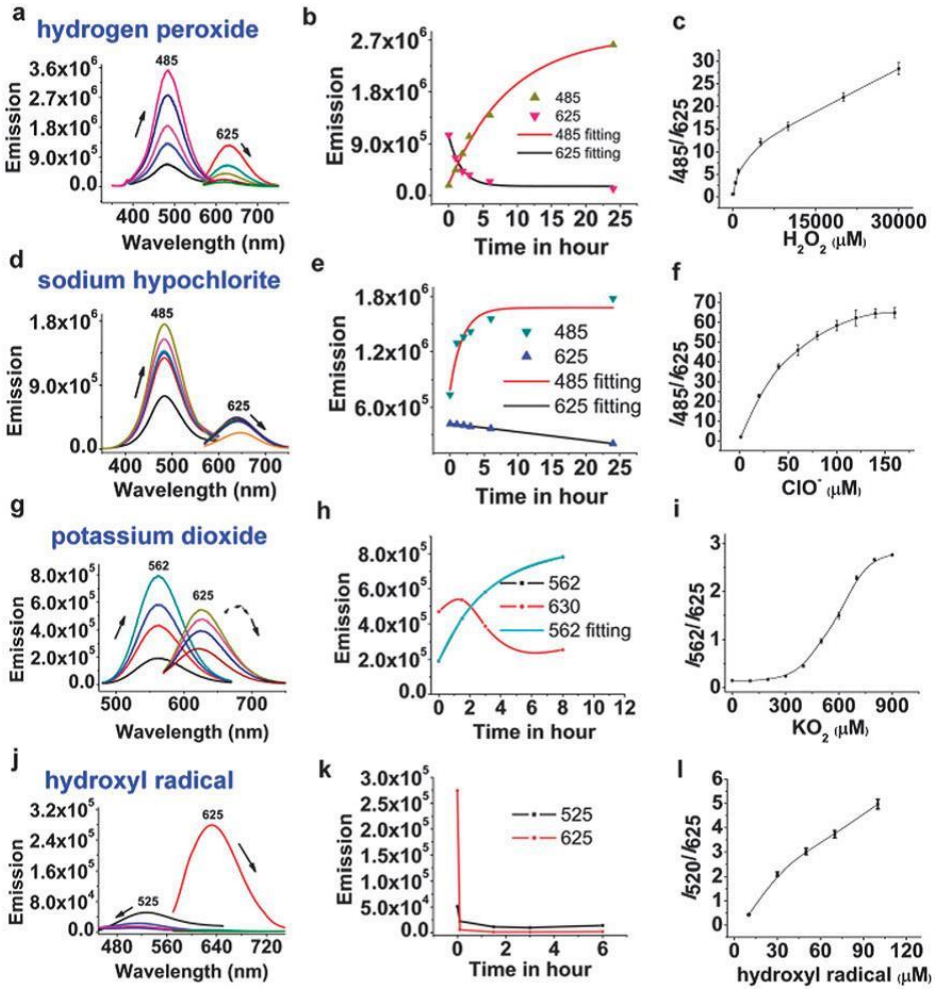

Figure 2. Selective oxidization of silver nanodots with reactive oxygen species. Figures in the first column show the spectral shifts of red C24 AgNDs in the presence of 1 mM hydrogen peroxide (a), 50 μM sodium hypochlorite (d), 600 μM potassium dioxide (g) and 30 μM hydroxyl radical (j). Their corresponding plots of intensity versus time are displayed in the second column, respectively. Given the ratiometric responses of C24 AgNDs to oxidizing agents, calibration curves of the respective ROS are shown in the third column. The arrows indicate the intensity changes with time. The solid lines in (b, e, h) as marked xxx fitting are tentative monoexponential fits of the time courses for the corresponding emission.

With another approach, the generation of new peaks was DNA sequence

dependent. Only loose single-stranded DNA protected AgNDs showed the selective oxidation to various color emitters. Oxidation of hairpin DNA-protected red AgNDs led to either the generation of the blue emitter, or the simple bleach of the red emission, as seen from another red emitter by hydrogen peroxide. Contrary to our expectation, the oxidants did not accelerate the formation of a specific emitter from its corresponding emissive precursor (one of red emitters). Such a phenomenon may suggest that the possible different oxidizing mechanisms, the difference in DNA sequences might also play a role. The precursors mentioned above have a mostly hairpin structure. The tight polycytosine loop that encapsulates AgNDs hinders the free rearrangement of silver cluster intermediates (Fig 3). However, the loose structures, such as polycytosine or 5'-CCCTAACTCCCC-3', provide enough protection during the somewhat free rearrangement of AgNDs.

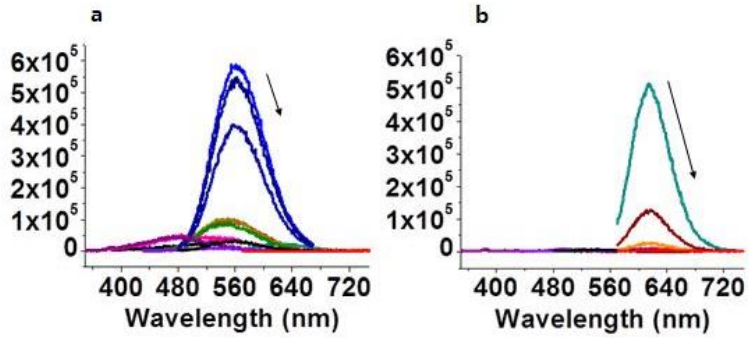

Figure 3. Different sequences of DNA encapsulated silver nanodots. Both of yellow emitter (λ_em= 560nm, 5'-ATATCCCCCCCCCCCCATAT-3)(a) and red emitter (λ_em=615nm, 5'-CGCGCCCCCCCCCGCG-3')(b) didn't show peak shift in the presence of 1mM hydrogen peroxide.

When red emitter is oxidized to blue emitter, their size got lowered and size distribution is also narrowed. HRTEM images of the red solution showed that the silver cluster/particle sizes ranged between 1.5nm to 8.5nm, with a higher distribution centered at 4.5nm (Figure 4b). It implies that the red is a spectrally pure, but chemically mixture, in which non-luminescent crystallites were easily observed. The oxidation of the red to the blue showed a much narrower distribution in size, with majority centered at 2.0nm (Figure 3c). Although particles in TEM images cannot be linked to emissive species directly, we could think that the oxidizing agents dramatically decreased the Ag cluster/nanoparticle size, and the size distribution reflected the change in cluster size between the red and the blue. Moreover, The ROS supposed to be able to remove not most non-luminescent silver clusters. That's why we can get spectrally-pure blue, exhibited strong absorption between 300nm and 450nm, with a quantum yield of 43% (Figure. 3a).

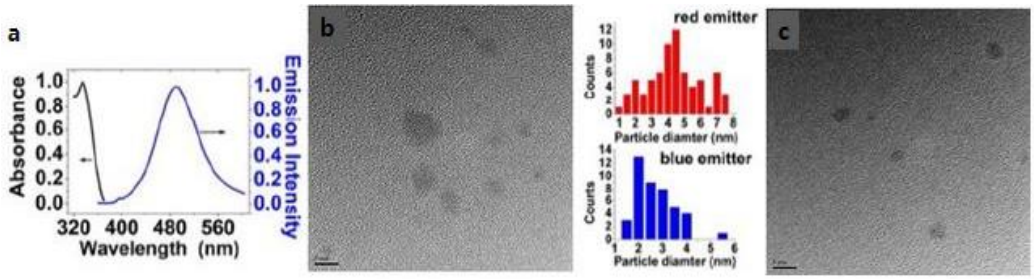

Figure 4. Characterization of the blue silver nanodot. (a) Absorption (black) and emission (blue) spectra of the blue silver nanodot. (b) HRTEM images of the as-prepared red emitter solution (left) and the corresponding H_2 O_2-oxidized blue emitter solution (right). The particle size distributions are displayed in the middle with the top for the red emitter and the bottom for the blue emitter. Scale bar: 5 nm

Being generated by oxidation, the blue Ag NDs is naturally stable in oxidizing environments. This property is valuable to the development of oxidant-resistant imaging agents. Here we compared blue emitter's photostability to organic dyes, Harmaline and Hoechst 33258, which have similar region of emission wavelength. In aqueous solution, harmaline was bleached instantly by sodium hypochlorite, but stable in 5mM hydrogen peroxide. However Hoechst 33258 was stable in both hydrogen peroxide and sodium hypochlorite solutions. For hoechst 33258 showed reasonably good photostability in ambient condition, we compared to photostabilities of in oxidized DNA-Ag NDs and Hoechst 33258 in the presence of hydrogen peroxide. Hoechst 33258 was reasonably stable, but quickly disappeared in the presence of hydrogen peroxide (Figure 5c and d). The H_2O_2 added blue Ag NDs, however, showed 4-fold better photostability than Hoechst 33258 (Figure 5a).

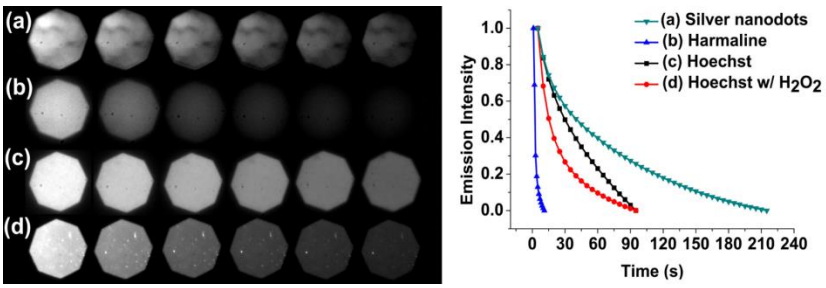

Figure 5. Comparison of the photostability of silver nanodots and blue dyes in oxidizing environments. (a-d) are the epifluorescence images of the H2O2-added blue silver nanodot, harmaline, Hoechst 33258 and Hoechst 33258 in the presence of H2O2, respectively. Samples were vacuum-dried in PVA film in the presence or absence of

hydrogen peroxide (5 mM). Images from left to right were taken after 5 s, 15 s, 25 s, 45 s, 65 s and 85 s exposure of UV excitation except harmaline after 1 s, 2 s, 4 s, 6 s, 8 s and 10 s UV light exposure. The plot of mean mission intensities of the above images indicates that silver nanodots are more stable in the presence of oxidizing agents.

As we can see from above results, the oxidized DNA-Ag NDs blue emitters have extremely good photostability in oxidation environment. It may be accounted for its positively charged silver clusters exhibit much better stability compared to the neutral in aqueous solution. One of the possible hypothesis is that the oxidizing agents degrade large size silver clusters, meanwhile, silver ions and even smaller non-luminescent clusters are generated. The deposit of silver ions on these small clusters at critical locations induces the formation of more stable charged species, and some of them are blue emitters. There is a report said that the deposition of silver ions on non-luminescent silver clusters might induce the formation of emissive Agn@Ag+ clusters.[108] Such a scenario was also supported by the fact that addition of a small amount of silver ions to the AgND solution increased the blue emission intensity.[86]

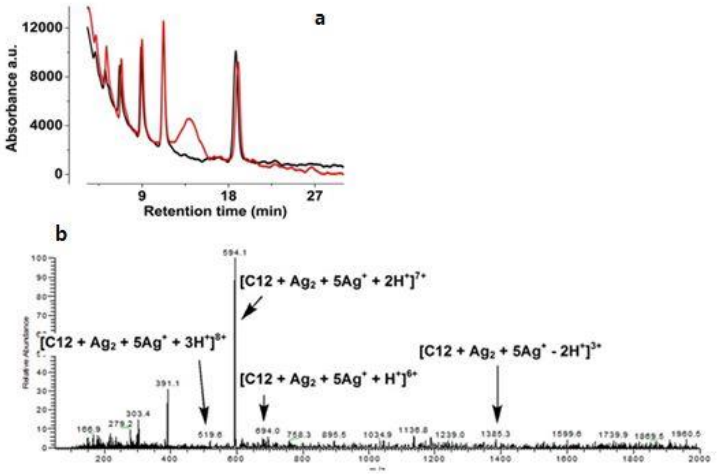

Figure 6. HPLC-UV chromatograph andMass spectrum of oxidized DNA-Ag NDs. (a) HPLC-UV chromatograph of the blue silver nanodot (red) and a mixture of C12 and silver ions (black). (b) ESI mass spectrum of the blue silver nanodot at retention time of 14 minutes shows the possible peaks of silver-DNA complexes.

What I want to deliver could be much clear with HPLC-MS spectrometry. A solution of the C12-protected blue Ag NDs alone exhibited an extra peak in HPLC spectrum (Figure 2c) which was absent in C12-protected red emitters and silver ions. The ESI mass spectrometry for the extra peak displayed spectra matching that of [C12-Ag2-5Ag+] (Figure 2d), which was likely the corresponding emitter.[109]

3.2. Ratiometric luminescence probe for hypochlorite detection

The dual-wavelength response of red Ag NDs was utilized for ratiometric

luminescence detection of a specific oxidant.[79] Here, the photoresponses of 24mer polycytosine-protected silver nanodots (red emitter, λ_{em}=625nm) upon the addition of sodium hypochlorite (NaOCl) are illustrated in Figure 7.

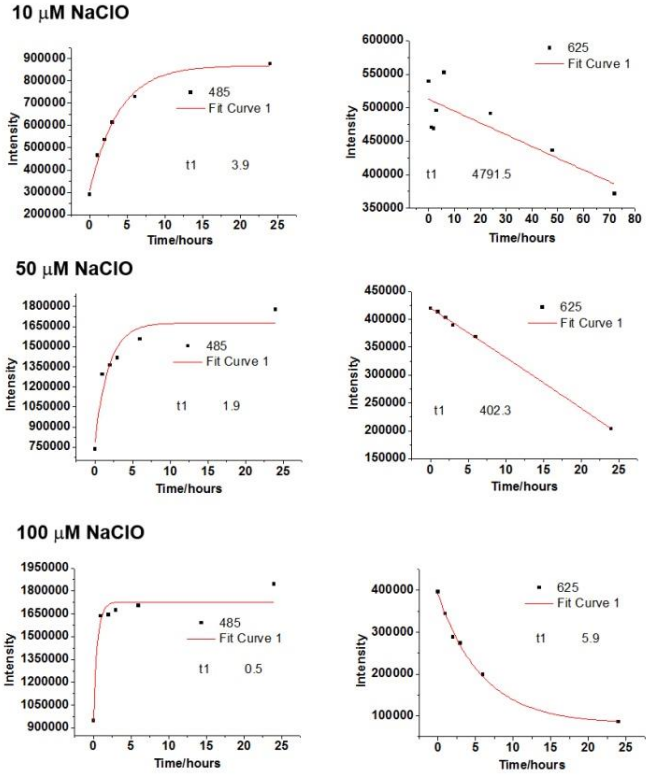

Figure 7. Reaction kinetics between red silver nanodots and sodium hypochlorite. The time course of C24-Ag silver nanodot emissions in the presence of 10, 50, and 100 μM of sodium hypochlorite. 485 and 625 indicate the wavelength at which the intensity was monitored. The red curves are tentative monoexponential fits of the time courses. The fitting indicates that the red emitters degraded much slower than the generation of the blue emitter.

The enhanced blue emission intensity levelled off at a certain point and

decreased gradually. Generally, increasing the concentrations of oxidants did not extend the maximum of blue emission intensity but just sped up the transition from red to the blue, leading to a fast response time towards the detection of oxidants.[110] One of the advantages of the ratiometric detection is that it can reduce the error to the density change of the probe. The I485/I625 ratios showed much less fluctuation at a given concentration of the oxidizing agent, comparing to direct detection of emission. (Figure 8).

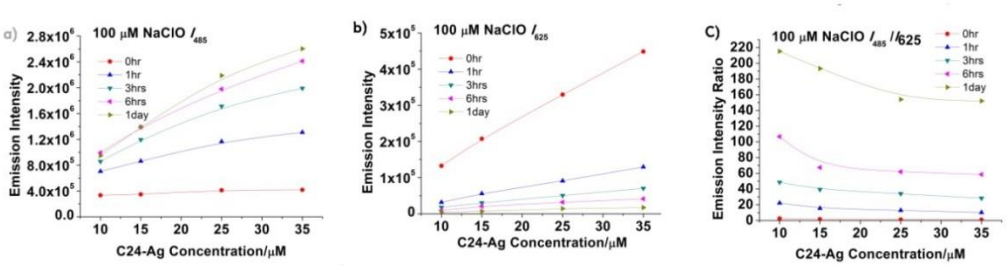

Figure 8. Emission and emission ratios of C24-Ag silver nanodots in the presence of 100μM of sodium hypochlorite. The emission was examined after the addition of an oxidant to the nanodots solutions. The higher the DNA-Ag NDs concentration, the stronger the emission. The I485/I625 ratios showed much less fluctuation at a given concentration of the oxidizing agent when the nanodots concentration varied between 15 to 35μM.

Some factors, such as pH and temperature, will influence the reaction rates between silver nanodots and oxidants, leading to change of the blue/red. The pH is important factor to successfully measure OCl^- in bio organisms. Our results (Figure 9) suggested that neutral solutions showed most consistent results. Therefore, we carried out all subsequent experimental conditions in pH 8 solutions at 25℃, which are potentially useful for further *in vivo* probe designing.

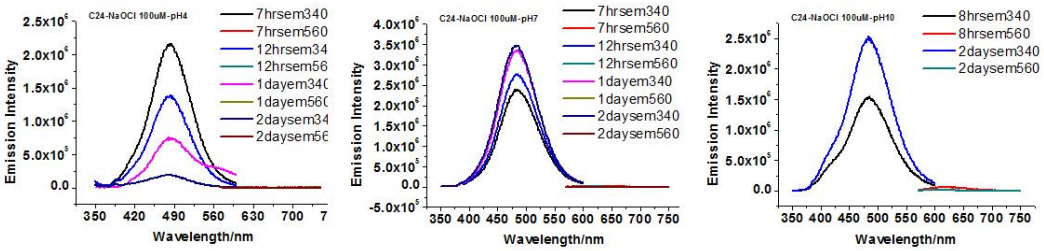

Figure 9. Influence of pH on the oxidization and stability of C24-Ag silver nanodots in the presence of 100μM of sodium hypochlorite. The emission intensity of 485 nm decreased at pH = 4 (left), but gradually increased at pH = 8 (middle) and pH = 10 (right). The numbers before "hrs" or "day" in the legends indicate the time to measure the emission and those after the 'em' indicate the excitation wavelengths.

Sodium hypochlorite is used widely in some cleaners as disinfectants and bleach. To accurately detect the hypochlorite concentration in household cleaners *in vitro*, we examined the influence of some salts and surfactants, and then we chose sodium sulfate and Triton X-100 as a basic builder in the calibration buffer for hypochlorite detection.

We chose four commercially-available cleaners marked as A to D. The

samples were diluted 6,000 folds into silver nanodots solutions. The photo-responses of the nanodots were recorded and the ratios of emission intensity I485/I625 were compared to a calibration curve of C24-Ag nanodots obtained from solutions with 5mM $NaSO_4$ and 10mM Triton X-100 at varied hypochlorite concentrations.

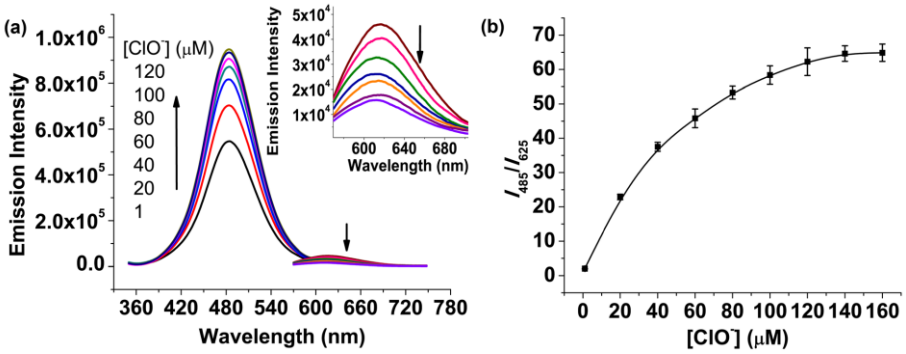

Figure 10. Luminescence titration of red silver nanodots with sodium hypochlorite. (a) Emission spectra were acquired 6 hrs after hypochlorite addition in 10 mM Triton X-100 and 5 mM sodium sulfate solution at pH 8.3. Inset: A close-up of the red regio of *I*485/*I*625 against OCl^- concentration. The error bars represent the standard errors.

Note that, the plot of luminescence intensity ratio of I_{485}/I_{625} against OCl^- concentration was not linear but leveled off at higher hypochlorite concentration. It can be partly explained by the contemporaneous generation and bleaching of the blue emitter both due to hypochlorite. The higher concentration of hypochlorite especially bleached the blue emitter faster, countervailing the increase of blue emission. Consequently, the detection region below 40μM of

hypochlorite was preferred in terms of better detection sensitivity. These cleaners contained 0.20M to 0.73M of hypochlorite. Some were lower than the recommended sodium hypochlorite concentrations in household bleach (5.25-6.15%) [111]. Our results were demonstrated by redox titrations of these samples based on the OCl^-/I_3^-/starch/$S_2O_3^{2-}$ method [112] (Table. 1), suggesting that our method is an excellent alternative for easy, fast and accurate hypochlorite detection.

Sample	A	B	C	D
Nanodot method (M)	0.23 ±0.01	0.73 ±0.05	0.20 ±0.02	0.20 ±0.01
Titrition method (M)	0.21 ±0.01	0.74 ±0.01	0.20 ±0.01	0.20 ±0.01

Table 1. **Detected hypochlorite concentrations in several commercially-available cleaners.**

3.3. Oxidant-resistant imaging by coupling with GOx

The successful association between the analyte and silver nanodots allowed us to primarily design probes for ultrasensitive detection with silver nanodots.

The low detection limits of AgNDs to ROS are potentially useful for such imaging purposes. However, it is impossible to highly-selectively detect ultra-

low concentration analyte under the current protocol. To overcome such a drawback, we coupled silver nanodots to glucose oxidase (GOx). The enzyme has been used as sensors for glucose and other analyte, in which hydrogen peroxide is generated as a signal transducer and colorimetrically,[113, 114] electrochemically,[115] chemiluminescently,[115] or fluorometrically visualized.[116] In our experiment, the ultralow limit of detection of GOx by silver nanodots enabled us to develop a protocol, in which the concentration of an analyte was correlated with the concentration of GOx. GOx consumed glucose to produce sufficient hydrogen peroxide, and the latter was subsequently visualized by the ratiometric response of our DNA-Ag NDs.

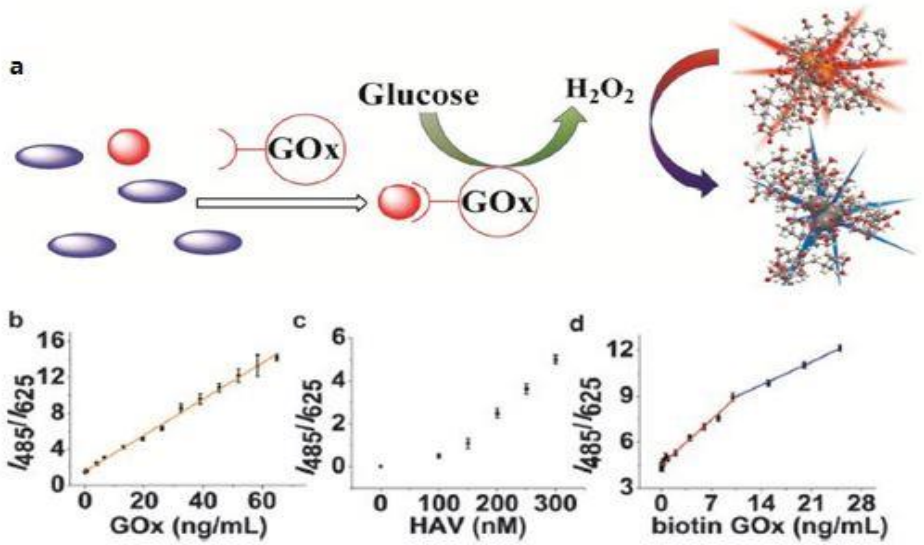

Figure 11. Visualization of glucose oxidase with red Ag NDs. (a) A schematic showing the coupling between GOx and Ag NDs for the detection of ultra-low concentration analyte. (b) Emission intensity ratio (I485/I625) of silver nanodots responding to the concentration of GOx. (c) The concentration of HAV DNA visualized

with red AgNDs after coupling the GOx and HAV DNA. (d) The detection efficiency of GOx improved when biotin–avidin pair was utilized for GOx collection.

This phenomenon was used for GOx visualization, with a detection limit of 400 pg mL^{-1} of GOx) (Figure 9b). Our protocol improved the detection limit by five orders compared to the QDs-based method,[117] in terms of the solution-based fluorometric detection of GOx. The ultralow detection limit of GOx was applied to develop AgND-based probes, for example, for a segment of hepatitis A virus (HAV) (Figure 9c). Moreover, when the binding between the analyte and GOx is strengthened, by utilizing the biotin–avidin pair, the detection limit has been dramatically improved (Figure 9d).

IV. Conclusions

In summary, the red and near-IR silver nanodots under loose single-stranded DNA protection were selectively oxidized to various emitters with blue, green or yellow emissions by reactive oxygen species. The blue emitter especially showed excellent chemical and photophysical stability, owing to its charged nature as shown from the HPLC-MS spectrometry. The kinetic data indicated that the intermediates from oxidation of the red and other non-emissive species led to the formation of the blue. Such a new controlled turn-on feature enabled us to

develop ratiometric luminescence probes and oxidant-resistant imaging agents.

We demonstrated dual-wavelength response of silver nanodots emitters as ratiometric probes to detect hypochlorite ions. In particular, we have demonstrated the availability of nanodots by monitoring the concentration of OCl^- inside several commercial cleaners.

In addition, silver nanodots were formulated to potentially detect any analyte with excellent selectivity and the limit of detection by coupling to glucose oxidase. Our results will not only greatly benefit the optical imaging in harsh oxidizing conditions, but also dramatically extended the scope of analytic application with silver nanodots.

V. References

1. P. M. Conn, *Essential Bioimaging Methods*, Academic Press, 2009.
2. J. M. Hoffman and S. S. Gambhir, *Radiology*, 2007, 244, 39-47.
3. H. R. Herschman, *Science*, 2003, 302, 605-608.
4. J. L. Prince and J. M. Links, *Medical imaging signals and systems*, Pearson Prentice Hall Upper Saddle River, NJ, 2006.
5. S. Ng, T. Chang, S. Ko, P. Yen, Y. Wan, L. Tang and M. Tsai, *Neuroradiology*, 1997, 39, 741-746.
6. D. H. Kraus, C. E. Lanzieri, J. R. Wanamaker, J. R. Little and P. Lavertu, *The Laryngoscope*, 1992, 102, 623-629.
7. M. E. Shenton, C. C. Dickey, M. Frumin and R. W. McCarley, *Schizophrenia research*, 2001, 49, 1-52.
8. R. Weissleder and U. Mahmood, *RADIOLOGY-OAK BROOK IL-*, 2001, 219, 316-333.
9. S. S. Y. Sanjiv Sam Gambhir, *Molecular Imaging with Reporter Genes*, Cambridge university press, May 2010.
10. S. M. Ametamey, M. Honer and P. A. Schubiger, *Chemical Reviews*, 2008, 108, 1501-1516.
11. H. Kobayashi, M. Ogawa, R. Alford, P. L. Choyke and Y. Urano, *Chemical Reviews*, 2009, 110, 2620-2640.

12. Z.-H. Cho, J. P. Jones and M. Singh, *Foundations of medical imaging*, Wiley New York:, 1993.
13. P. J. Early and D. B. Sodee, *Principles and practice of nuclear medicine*, Mosby Inc, 1995.
14. G. Alexandrakis, F. R. Rannou and A. F. Chatziioannou, *Physics in medicine and biology*, 2005, 50, 4225.
15. T. F. Massoud and S. S. Gambhir, *Genes & development*, 2003, 17, 545-580.
16. M. E. Phelps, *Proceedings of the National Academy of Sciences*, 2000, 97, 9226-9233.
17. D. T. Cramb, *The Journal of Physical Chemistry Letters*, 2013, 4, 2242-2243.
18. A. Gibson, J. Hebden and S. R. Arridge, *Physics in medicine and biology*, 2005, 50, R1.
19. R. L. Barbour, H. L. Graber, Y. Pei, S. Zhong and C. H. Schmitz, *JOSA A*, 2001, 18, 3018-3036.
20. D. A. Boas, D. H. Brooks, E. L. Miller, C. A. DiMarzio, M. Kilmer, R. J. Gaudette and Q. Zhang, *Signal Processing Magazine, IEEE*, 2001, 18, 57-75.
21. R. Weissleder and M. J. Pittet, *Nature*, 2008, 452, 580-589.
22. H. Xu, Q. Li, L. Wang, Y. He, J. Shi, B. Tang and C. Fan, *Chem. Soc. Rev.*, 2014.
23. D. M. Close, S. S. Patterson, S. Ripp, S. J. Baek, J. Sanseverino and G. S. Sayler, *PLoS One*, 2010, 5, e12441.
24. K. L. Kelly, E. Coronado, L. L. Zhao and G. C. Schatz, *The Journal of Physical Chemistry B*, 2003, 107, 668-677.

25. E. M. Goldys, *Fluorescence applications in biotechnology and life sciences*, John Wiley & Sons, 2009.

26. K. M. Berland, P. So and E. Gratton, *Biophysical journal*, 1995, 68, 694-701.

27. R. Rigler, *Journal of biotechnology*, 1995, 41, 177-186.

28. K. Licha, in *Contrast Agents Ii*, Springer, 2002, pp. 1-29.

29. J. L. Kovar, M. A. Simpson, A. Schutz-Geschwender and D. M. Olive, *Biochemistry--Faculty Publications*, 2007, 9.

30. T. V. Truong, W. Supatto, D. S. Koos, J. M. Choi and S. E. Fraser, *Nature methods*, 2011, 8, 757-760.

31. R. Weissleder, C.-H. Tung, U. Mahmood and A. Bogdanov, *Nature biotechnology*, 1999, 17, 375-378.

32. D. M. Shotton, *Journal of Cell Science*, 1989, 94, 175-206.

33. T. Wilson, *Confocal microscopy*, Academic Press London, 1990.

34. M. Rajadhyaksha, S. González, J. M. Zavislan, R. R. Anderson and R. H. Webb, *Journal of Investigative Dermatology*, 1999, 113, 293-303.

35. T. Pittman, Y. Shih, D. Strekalov and A. Sergienko, *Physical Review A*, 1995, 52, R3429.

36. F. Helmchen and W. Denk, *Nature methods*, 2005, 2, 932-940.

37. B. R. Masters, P. So and E. Gratton, *Biophysical journal*, 1997, 72, 2405-2412.

38. Y. Ooyama, A. Matsugasako, K. Oka, T. Nagano, M. Sumomogi, K. Komaguchi, I. Imae and Y. Harima, *Chem. Commun.*, 2011, 47, 4448-4450.

39. V. Ntziachristos, J. Ripoll, L. V. Wang and R. Weissleder, *Nature biotechnology*,

2005, 23, 313-320.

40. P. W. Atkins and J. De Paula, *Oxford*, 1998.

41. S. E. Braslavsky, *Pure and Applied Chemistry*, 2007, 79, 293-465.

42. B. Valeur and M. N. Berberan-Santos, *Journal of Chemical Education*, 2011, 88, 731-738.

43. P. Milonni, in *The Wave-Particle Dualism*, Springer, 1984, pp. 27-67.

44. J. W. Lichtman and J.-A. Conchello, *Nature Methods*, 2005, 2, 910-919.

45. J. H. Moore Jr, *Physical Review A*, 1973, 8, 2359.

46. N. J. Turro, *Modern molecular photochemistry*, University Science Books, 1991.

47. W. Moerner and L. Kador, *Physical Review Letters*, 1989, 62, 2535.

48. M. Orrit and J. Bernard, *Physical Review Letters*, 1990, 65, 2716.

49. L. Angelova, E. Borisova, A. Zhelyazkova, M. Keremedchiev, B. Vladimirov and L. Avramov, 2013.

50. D. Wang and T. Imae, *Journal of the American Chemical Society*, 2004, 126, 13204-13205.

51. M. Monici, *Biotechnology annual review*, 2005, 11, 227-256.

52. A. P. Demchenko, *Introduction to Fluorescence Sensing*, 2009.

53. V. Ntziachristos, J. Ripoll and R. Weissleder, *Optics letters*, 2002, 27, 333-335.

54. P. M. Bendix, M. S. Pedersen and D. Stamou, *Proceedings of the National Academy of Sciences*, 2009, 106, 12341-12346.

55. J. Widengren and R. Rigler, *Bioimaging*, 1996, 4, 149-157.

56. U. Resch-Genger, M. Grabolle, S. Cavaliere-Jaricot, R. Nitschke and T. Nann,

Nature methods, 2008, 5, 763-775.

57. A. Vonarbourg, C. Passirani, P. Saulnier and J.-P. Benoit, *Biomaterials*, 2006, 27, 4356-4373.

58. L. Rajendran, H.-J. Knölker and K. Simons, *Nature Reviews Drug Discovery*, 2010, 9, 29-42.

59. V. P. Torchilin, *Annu. Rev. Biomed. Eng.*, 2006, 8, 343-375.

60. B. C. Dickinson and C. J. Chang, *Nature chemical biology*, 2011, 7, 504-511.

61. X. Michalet, F. Pinaud, L. Bentolila, J. Tsay, S. Doose, J. Li, G. Sundaresan, A. Wu, S. Gambhir and S. Weiss, *Science*, 2005, 307, 538-544.

62. R. Weissleder, *Radiology*, 1999, 212, 609-614.

63. Q. Shao and B. Xing, *Chem. Soc. Rev.*, 2010, 39, 2835-2846.

64. T. Vosch, Y. Antoku, J.-C. Hsiang, C. I. Richards, J. I. Gonzalez and R. M. Dickson, *Proceedings of the National Academy of Sciences*, 2007, 104, 12616-12621.

65. W. Liu, M. Howarth, A. B. Greytak, Y. Zheng, D. G. Nocera, A. Y. Ting and M. G. Bawendi, *Journal of the American Chemical Society*, 2008, 130, 1274-1284.

66. A. Sukhanova, J. Devy, L. Venteo, H. Kaplan, M. Artemyev, V. Oleinikov, D. Klinov, M. Pluot, J. H. Cohen and I. Nabiev, *Analytical biochemistry*, 2004, 324, 60-67.

67. W. C. Chan and S. Nie, *Science*, 1998, 281, 2016-2018.

68. S. Choi, R. M. Dickson and J. H. Yu, *Chem. Soc. Rev.*, 2012, 41, 1867-1891.

69. J. T. Petty, J. Zheng, N. V. Hud and R. M. Dickson, *Journal of the American*

Chemical Society, 2004, 126, 5207-5212.

70. J. Zheng and R. M. Dickson, *Journal of the American Chemical Society*, 2002, 124, 13982-13983.

71. A. Henglein, *Chemical Reviews*, 1989, 89, 1861-1873.

72. Z. Shen, H. Duan and H. Frey, *Advanced Materials*, 2007, 19, 349-352.

73. J. Yu, S. A. Patel and R. M. Dickson, *Angewandte Chemie*, 2007, 119, 2074-2076.

74. S. Choi, J. Yu, S. A. Patel, Y.-L. Tzeng and R. M. Dickson, *Photochemical & Photobiological Sciences*, 2011, 10, 109-115.

75. I. Díez, M. Pusa, S. Kulmala, H. Jiang, A. Walther, A. S. Goldmann, A. H. Müller, O. Ikkala and R. H. Ras, *Angewandte Chemie International Edition*, 2009, 48, 2122-2125.

76. J. Yu, S. Choi and R. M. Dickson, *Angewandte Chemie*, 2009, 121, 324-326.

77. W. Guo, J. Yuan, Q. Dong and E. Wang, *Journal of the American Chemical Society*, 2009, 132, 932-934.

78. S. A. Patel, C. I. Richards, J.-C. Hsiang and R. M. Dickson, *Journal of the American Chemical Society*, 2008, 130, 11602-11603.

79. C. I. Richards, S. Choi, J. C. Hsiang, Y. Antoku, T. Vosch, A. Bongiorno, Y. L. Tzeng and R. M. Dickson, *Journal of the American Chemical Society*, 2008, 130, 5038-5039.

80. H.-C. Yeh, J. Sharma, J. J. Han, J. S. Martinez and J. H. Werner, *Nano letters*, 2010, 10, 3106-3110.

81. Y. Antoku, J.-i. Hotta, H. Mizuno, R. M. Dickson, J. Hofkens and T. Vosch, *Photochemical & Photobiological Sciences*, 2010, 9, 716-721.

82. D. Schultz and E. G. Gwinn, *Chemical Communications*, 2012, 48, 5748-5750.

83. J. T. Petty, S. P. Story, J.-C. Hsiang and R. M. Dickson, *The journal of physical chemistry letters*, 2013, 4, 1148-1155.

84. D. Nykypanchuk, M. M. Maye, D. van der Lelie and O. Gang, *Nature*, 2008, 451, 549-552.

85. L. Sohncke, *Nature*, 1884, 29, 383-384.

86. C. M. Ritchie, K. R. Johnsen, J. R. Kiser, Y. Antoku, R. M. Dickson and J. T. Petty, *The Journal of Physical Chemistry C*, 2007, 111, 175-181.

87. Y. W. Yap, M. Whiteman and N. S. Cheung, *Cellular signalling*, 2007, 19, 219-228.

88. D. I. Pattison, C. L. Hawkins and M. J. Davies, *Biochemistry*, 2007, 46, 9853-9864.

89. P. S. Green, A. J. Mendez, J. S. Jacob, J. R. Crowley, W. Growdon, B. T. Hyman and J. W. Heinecke, *J. Neurochem.*, 2004, 90, 724.

90. J. W. Heinecke, *The American journal of cardiology*, 2003, 91, 12-16.

91. K. MiáLee, Y. YeongáSeo, H. KyoungáChoi, H. NaáKim, M. JungáKim and S. YoungáLee, *Chemical Communications*, 2011, 47, 4373-4375.

92. M. Benhar, D. Engelberg and A. Levitzki, *EMBO Rep.*, 2002, 3, 420.

93. A. L. Jackson and L. A. Loeb, *Mutation Research/Fundamental and Molecular Mechanisms of Mutagenesis*, 2001, 477, 7-21.

94. M. R. Ramsey and N. E. Sharpless, *Nature cell biology*, 2006, 8, 1213-1215.

95. F. L. Richter and B. R. Cords, *Disinfection, Sterilization and Preservation. 5th ed. Philadelphia: Lippincott Williams & Wilkins*, 2001, 473-487.

96. J. R. Haag and R. G. Gieser, *JAMA: The Journal of the American Medical Association*, 1983, 249, 2507-2508.

97. T. A. Ingram III, *Journal of endodontics*, 1990, 16, 235-238.

98. G. D. LANDAU and W. H. SAUNDERS, *Archives of Otolaryngology—Head & Neck Surgery*, 1964, 80, 174.

99. E. A. Podrez, H. M. Abu-Soud and S. L. Hazen, *Free Radical Biology and Medicine*, 2000, 28, 1717-1725.

100. J. Raba and H. A. Mottola, *Critical reviews in Analytical chemistry*, 1995, 25, 1-42.

101. R. Kohen, *Biomedicine & pharmacotherapy*, 1999, 53, 181-192.

102. X. Chen, X. Tian, I. Shin and J. Yoon, *Chem. Soc. Rev.*, 2011, 40, 4783-4804.

103. E. W. Miller, O. Tulyathan, E. Y. Isacoff and C. J. Chang, *Nature chemical biology*, 2007, 3, 263-267.

104. T. Finkel, *Current opinion in cell biology*, 2003, 15, 247-254.

105. J. R. Stone and S. Yang, *Antioxidants & redox signaling*, 2006, 8, 243-270.

106. L. J. Kirsch, D. A. Parkes, D. J. Waddington and A. Woolley, *Journal of the Chemical Society, Faraday Transactions 1: Physical Chemistry in Condensed Phases*, 1978, 74, 2293-2300.

107. W. M. Haynes, D. R. Lide and T. J. Bruno, *CRC Handbook of Chemistry and*

Physics 2012-2013, CRC press, 2012.

108. M. Treguer, F. Rocco, G. Lelong, A. Le Nestour, T. Cardinal, A. Maali and B. Lounis, *Solid state sciences*, 2005, 7, 812-818.

109. M. V. Shestakov, N. T. Cuong, V. K. Tikhomirov, M. T. Nguyen, L. F. Chibotaru and V. V. Moshchalkov, *The Journal of Physical Chemistry C*, 2013, 117, 7796-7800.

110. S. Choi, S. Park, K. Lee and J. Yu, *Chemical Communications*, 2013, 49, 10908-10910.

111. W. A. Rutala, D. J. Weber and C. f. D. Control, *Guideline for Disinfection and Sterilization in Healthcare Facilities, 2008*, Centers for Disease Control (U.S.), 2008.

112. D. S. Jackson, D. F. Crockett and K. A. Wolnik, *Journal of forensic sciences*, 2006, 51, 827-831.

113. J. Middleton and W. Griffiths, *British medical journal*, 1957, 2, 1525.

114. J. Okuda, I. Miwa, K. Maeda and K. Tokui, *Carbohydrate research*, 1977, 58, 267-270.

115. G. G. Guilbault, B. C. Tyson Jr, D. Kramer and P. L. Cannon Jr, *Analytical Chemistry*, 1963, 35, 582-586.

116. M. Wu, Z. Lin, M. Schäferling, A. Dürkop and O. S. Wolfbeis, *Analytical biochemistry*, 2005, 340, 66-73.

117. L. Saa and V. Pavlov, *Small*, 2012, 8, 3449-3455.

국문초록

형광 현미경은 최적화된 시스템에서 단일 분자까지 검출할 수 있는 높은 감도와 선택성, 시간분해능을 갖기 때문에, 이를 생체 분자 영상에 적용하기 위한 개발이 지속적으로 이루어지고 있다. 형광 현미경에서 최적의 효과를 달성하기 위해서는 적절한 형광 탐침을 선택하는 것이 필수적이다. 단일 사슬 DNA 로 둘러싸인 은 나노닷은 뛰어난 광물리적 특성과 함께 적절한 생체적합성을 가졌기 때문에 최근 크게 주목 받고 있다. 그러나 DNA−은 나노닷은 내부 구조와 반응 메커니즘이 명확히 밝혀지지 않았다. 따라서 다양한 산화 과정에서 나타나는 DNA−은 나노닷의 특성을 분석하여 이 물질에 대해 이해할 수 있는 실마리를 얻고자 한다. 우리는 다양한 종류의 활성산소종을 이용하여 붉은 색 빛을 발하는 DNA−은 나노닷을 산화시켜 산화 특성을 조사 하였다. 또한 발견된 산화특성을 이용해서 비율척도 발광 탐침 및 새로운 형태의 생체 영상 방법을 개발하였다.

주요어 : DNA, 은 나노닷, 비율척도, 과산화수소, 차아염소산염, 글루코오스 산화효소

학번 : 2011-21578